Spectral holes and induced luminescence in KCl co-doped with Eu^{2+} and Eu^{3+} ions

2001 J. Phys.: Condens. Matter 13 2835

(http://iopscience.iop.org/0953-8984/13/12/308)

INSTITUTE OF PHYSICS PUBLISHING JOURNAL OF PHYSICS: CONDENSED MATTER

J. Phys.: Condens. Matter **13** (2001) 2835–2843 www.iop.org/Journals/cm PII: S0953-8984(01)19233-7

Spectral holes and induced luminescence in KCl co-doped with Eu^{2+} and Eu^{3+} ions

Jun-Gill Kang[1], **Jae-Sun Jung, Jung-Pyo Hong, Seok-Jae Won, Youngku Sohn and Choong Kyun Rhee**

Department of Chemistry, Chungnam National University, Taejeon, 305-764, Korea

E-mail: jgkang@cuvic.cnu.ac.kr

Received 21 November 2000, in final form 15 January 2001

Abstract

The luminescence spectrum of KCl co-doped with divalent and trivalent europium ions was measured as a function of temperature in order to characterize novel spectral holes that appear in the blue emission from Eu^{2+}. The radiative energy transfer from Eu^{2+} to Eu^{3+} produces the spectral holes and induces the luminescence from Eu^{3+} responsible for the $^5D_0 \rightarrow {}^7F_J$ ($J = 0$, 1, 2, 3, 4) transitions. The holes and the induced luminescence are strongly associated with the thermal band broadening of the blue emission. In addition, the observed line splitting of the induced luminescence of Eu^{3+} is also discussed in terms of a crystal-field Hamiltonian.

1. Introduction

Recently, persistent spectral hole burning (PSHB) phenomena have been observed in Sm^{2+} and Eu^{3+} ions in sol–gel derived glass (Nogami *et al* 1995, Fujita *et al* 1997, Nogami 1999, Buddhuda *et al* 1999). Both ions are isoelectronic, with a $4f^6$ configuration, of which the lowest and first excited states are non-degenerate $^7F_0$ and $^5D_0$, respectively. Using irradiation with a narrow-band laser, spectral holes were burnt in the $^7F_0 \rightarrow {}^5D_0$ excitation of both ions. The $^5D_0 \rightarrow {}^7F_0$ luminescent transition is in principle forbidden by the electric-dipole selection rule, but this transition may increase its intensity through J mixing under low site symmetry, such as C_s, C_n and C_{nv}. However, the intensity of this transition is still very low compared with those of the $^5D_0 \rightarrow {}^7F_J$ (1, 2, 4) transitions. The weak depth of the hole is difficult to incorporate into commercial systems.

Previously, we observed a series of distinct spectral holes in the blue emission from KCl co-doped with divalent and trivalent europium ions (Kang *et al* 2000a). The blue emission, attributed to the $5d \rightarrow 4f$ transition of Eu^{2+}, is very bright. Spectral holes do not appear in KCl doped with divalent europium ion alone. This suggests that the spectral holes in the blue emission could be due to radiative energy transfer from Eu^{2+} to Eu^{3+}. The main purpose of this work was to characterize the spectral holes in the blue emission from Eu^{2+} centres and

[1] To whom all correspondence should be addressed.

0953-8984/01/122835+09$30.00

the induced luminescence from Eu^{3+} centres as a function of temperature. The crystal-field potential plays a key role in characterizing the intensity and band splitting of the luminescence of Eu^{3+}. The observed line splitting in the $^5D_0 \rightarrow {}^7F_J$ transitions was analysed with the aid of the crystal-field potential on the basis of the site symmetry of the Eu(III) ion in the complex. In this paper, we also clearly assign the luminescence and electronic energy-level structure of the ^7F_J states by simulating phenomenological crystal-field splitting.

2. Experiment

The sample used in this work is the same as sample C described earlier (Kang *et al* 2000a). Opaque crystals were obtained using the vertical Bridgeman method, after baking a mixture of KCl (99.99+%, Aldrich) and anhydrous $EuCl_3$ (99.9+%, Aldrich) at 500 °C in air.

To measure the temperature dependence of the luminescence spectrum, a sample of appropriate size was placed on the cold finger of an ADP cryostat. Excited light from a He–Cd laser was focused on the sample. The luminescence spectrum was measured at a 90° angle with a SPEX double monochromator equipped with a SPEX L-N_2 cooled CCD. The induced luminescence spectrum due to the radiative transfer was recorded with an Oriel 1000 W Xe arc lamp and an Oriel MS257 monochromator, as described elsewhere (Kang *et al* 2000b).

3. Results and discussion

3.1. Emission from Eu^{2+}

As shown in figure 1, the 325 nm excitation produced a very strong, wide band peaking at 422 nm, and a series of very sharp lines in the visible region at room temperature. The bright blue emission has been attributed to the $^2T_{2g}(4f^6 5d) \rightarrow {}^8S_{7/2}(4f^7)$ transition of divalent europium ion (Rubio 1991, Kang *et al* 2000b). The series of sharp lines in the visible region apparently accounts for the $^5D_0 \rightarrow {}^7F_J$ ($J = 0$–4) transitions of trivalent europium ion in the KCl host. The characteristic feature in the blue emission is the five distinct spectral holes, peaking at 23 914, 24 075, 24 171, 24 308, and 24 378 cm^{-1} (labelled holes 1, 2, 3, 4 and 5, respectively, in order of increasing energy). It is worthwhile noting that the wavelengths of hole positions and peaks of the $^7F_0 \rightarrow {}^5D_3$ transition, reported previously, should be reduced by ~1.5 nm, because the two monochromators used previously were red-shifted by accident. The half widths of the five holes ranged from 5 to 30 cm^{-1} at room temperature. Of the five holes, hole 1 has the widest bandwidth and hole 2 is the deepest. Previously, we found that the positions of these peaks correspond exactly to the location of the $^7F_0 \rightarrow {}^5D_3$ transitions of the trivalent europium ion (Kang *et al* 2000a). Furthermore, these spectral holes did not appear in KCl doped only with Eu^{2+}. These results previously led us to assume that the extraordinary feature appeared via the process of reabsorption from Eu^{2+} to Eu^{3+} ions in KCl. In this work, luminescence spectra from KCl co-doped with Eu^{2+} and Eu^{3+} excited at 325 nm were measured at various temperatures. It should be noted that the depth of the hole depends on the position of the excitation beam spot on the crystals. Depending on the beam spot on the crystal surface, hole 1 was not produced. Some results, obtained from the best position of the crystals, are shown in figure 2.

The intensity and bandwidth of the 422 nm emission band decrease with decreasing temperature, but become constant at below 100 K. The thermal vibrations of the lattice, which cause the thermal broadening, are very effective at above 100 K. At low temperatures, multiphonon or vibronic relaxation may not make any relative contributions to the bandwidth.

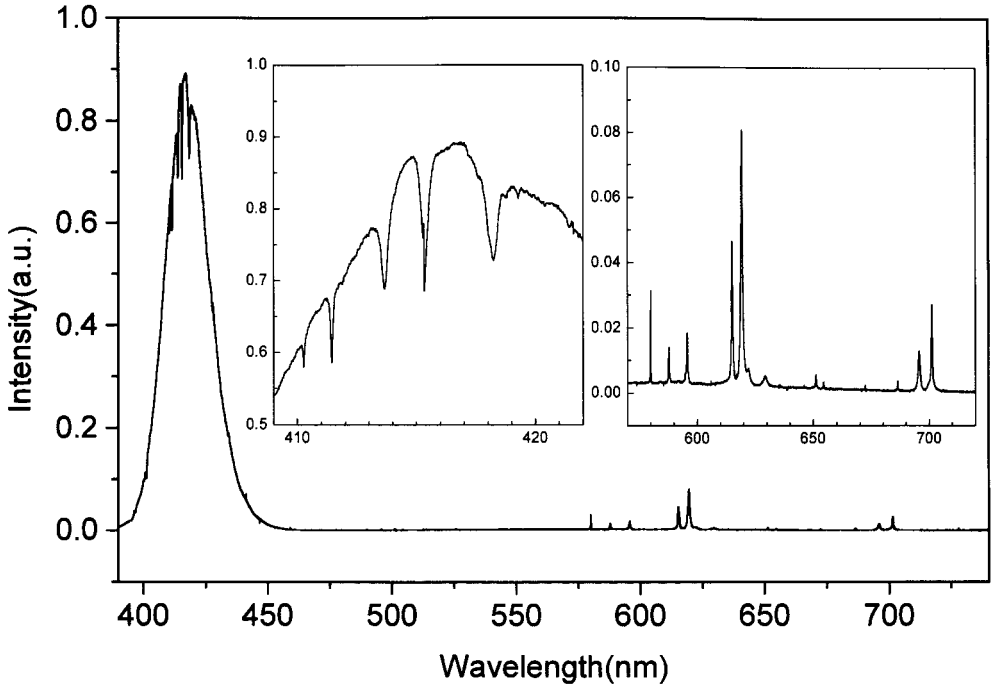

Figure 1. The luminescence spectrum from KCl co-doped with Eu^{2+} and Eu^{3+} ions ($\lambda_{exc} = 325$ nm and $T = 300$ K).

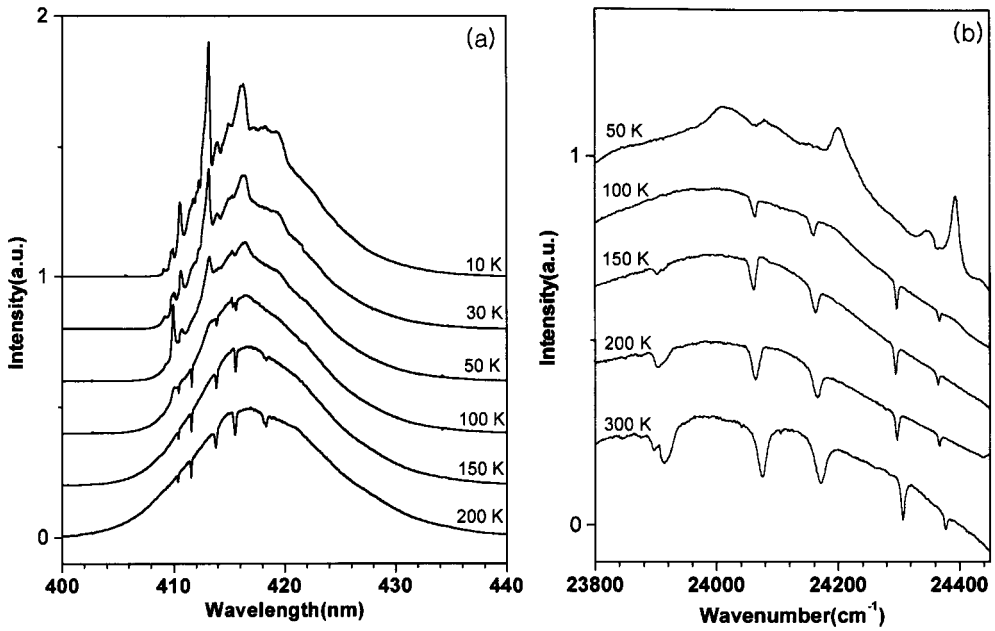

Figure 2. The luminescence band from Eu^{2+} measured at various temperatures (a) and spectral holes in the extended scale (b).

There is experimental evidence for thermally quenched multiphonon or vibronic relaxation at low temperature in the appearance of more than three lines peaking at 24 393 cm^{-1} (410.0 nm), 24 202 cm^{-1} (413.2 nm) and 24 011 cm^{-1} (416.5 nm) in the blue emission band at 50 K. As the temperature falls, the last two lines become increasingly intense. As shown in figure 2(a), the last two lines are very sharp at $T = 10$ K. These lines in the emission spectrum can be regarded as the zero-phonon lines of the $^2T_{2g}(4f^6 5d) \rightarrow {}^8S_{7/2}(4f^7)$ transition. The 422 nm emission from Eu^{2+} in KCl consists of several Gaussian components. These several zero-phonon lines may be strongly associated with the complexity of the Eu^{2+} ion in the excited state in KCl. Previously, we investigated the polarization of the 422 nm emission from KCl:Eu^{2+} (Kang *et al* 2000b). The characteristic features in the 422 nm emission are the unusual polarization, multiple components, the strong Stokes shift and the widened bandwidth. According to the theoretical treatment for the threefold $^2T_{2g}(xy, yz, zx)$ state, the Jahn–Teller and spin–orbit interactions play key roles in the optical process. The Jahn–Teller effect coupled to the tetragonal $E_g(Q_2, Q_3)$ mode, which predominates over the coupling with the trigonal $T_{2g}(Q_4, Q_5, Q_6)$ mode, results in three tetragonal T minima (T_{xy}, T_{yz}, T_{zx}) on the $^2T_{2g}$ paraboloids in (Q_2, Q_3) space. The Jahn–Teller effect splits the threefold degenerate state into the twofold degenerate E state at low energy and the non-degenerate A state at high energy. Spin–orbit coupling may cause mixing of the three mutually orthogonal paraboloids, resulting in two kinds of minimum on each paraboloid. An additional tetragonal T* minimum $(T^*_{xy}, T^*_{yz}, T^*_{zx})$ can coexist in the opposite direction to the T minima. In addition, the perturbing effect arising from the charge compensating cation vacancy (CCV, v_c^-) may cause further splitting of the doubly degenerate T and T* minima, depending on the relative orientations of the JTE and CCV (Kang 2000b). According to this energy-level scheme, the observed zero-phonon lines are attributed to the zero-phonon transitions from these minima coexisting on the APES of the $^2T_{2g}$ state.

The temperature dependence of the spectral holes is similar to the thermal quenching of the band broadening of the 422 nm emission. With decreasing temperature, the width and depth of the holes decrease. Hole 1 is strongly quenched and disappears below $T = 150$ K. The other holes also decrease, but they persist at lower temperatures, although as shown in the extended scale of figure 2(b), holes 2, 3, 4 and 5 only appear as traces at very low temperatures. If the spectral holes arise from the radiative energy transfer from the sensitizer (S) of Eu^{2+} to the activator (A) of Eu^{3+}, the temperature dependency of the holes may be relative to that of the luminescence of Eu^{3+}. We chose 340 nm to selectively excite Eu^{2+}. Without the Eu^{2+} sensitizer, this excitation cannot produce the sharp luminescence lines of the activator Eu^{3+}. As shown in figure 3, the band splitting and peak position of the luminescence of Eu^{3+}, induced by the energy transfer, are exactly the same as produced by the 325 nm excitation. For most Eu^{3+} complexes, the intensity of the luminescence increases with decreasing temperature. On the other hand, the intensities of the sharp lines of the induced luminescence decrease with decreasing temperature. Figure 4 plots the effect of temperature on the total area of the five holes and the intensity of the 619.8 nm line, which is the strongest induced luminescence line. As expected, both show similar exponential decays with respect to $1/T$. These results strongly support the hypothesis that the spectral holes in the blue emission from Eu^{2+} result from the radiative energy transfer from Eu^{2+} to Eu^{3+}, resulting in the $^4D_0 \rightarrow {}^7F_J$ luminescence lines from Eu^{3+}. The energy transfer from S to A may occur if a suitable interaction between the two electronic systems exists, such as an exchange, electrostatic or magnetic interaction (Dexter 1953, Reisfeld and Jørgensen 1977). The probability of energy transfer is proportional to the product of the square of the interaction matrix and the integral over the normalized emission band of S and the absorption band of A. The main difference between radiative and nonradiative energy transfer is that the former depends on the size and shape of the crystal and also on the

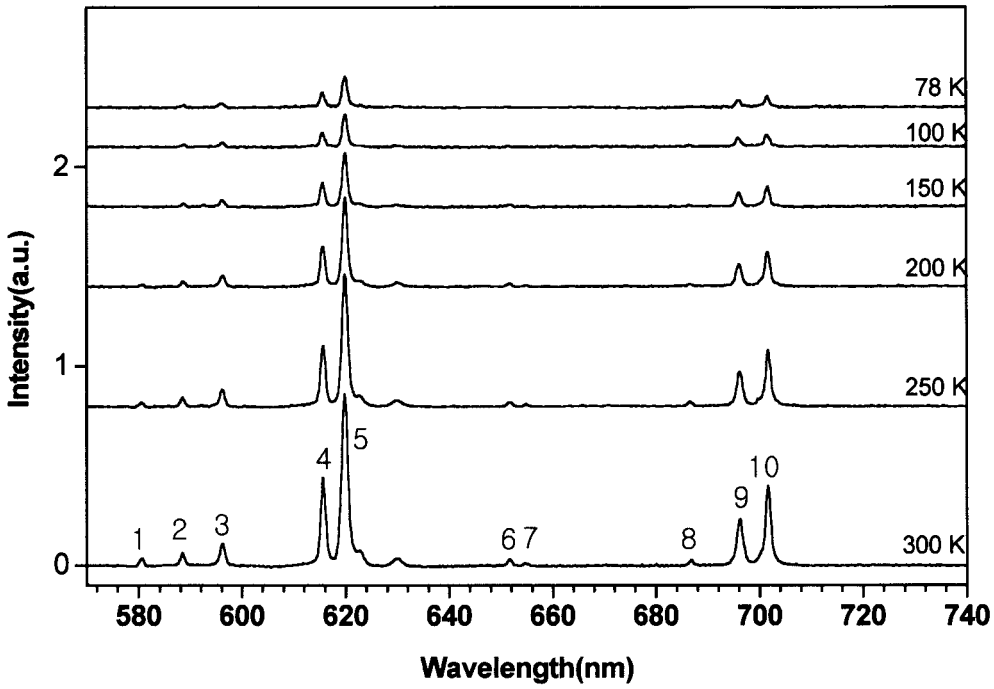

Figure 3. The induced luminescence spectrum from Eu^{3+} via reabsorption measured at various temperatures ($\lambda_{exc} = 340$ nm).

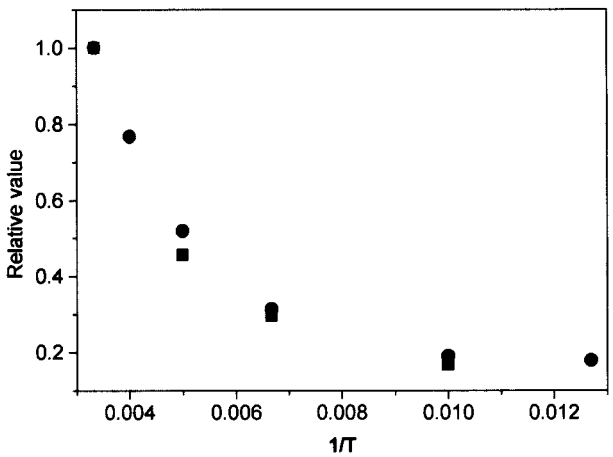

Figure 4. The ratios of hole areas and intensity of the 619.8 nm band to those measured at 300 K (circles: hole area, squares: intensity).

details of the overlap of the emission of S with the absorption of A. For the Eu^{2+}–Eu^{3+} system, however, other interaction between Eu^{2+} and Eu^{3+} would be expected from their electronic configurations in the excited state. Taking into account the fact that the 4f $\rightarrow$ 5d transition is allowed by the electric dipole moment and the 4f $\rightarrow$ 4f transition is allowed by the induced electric dipole moment due to the CF perturbation, the electric dipole-induced electric dipole

transfer could be very effective in the energy transfer from Eu^{2+} to Eu^{3+}. In general, great radiative transition can be expected at low temperature at which the bands become sharper and more intense in luminescence and in excitation. However, the observed temperature dependence on the bandwidths of the blue emission and the spectral holes suggests that the overlap may be strongly associated with the lattice vibration. In the energy matrix, spin selection rules for conserving the total spin of the system before and after the transfer must be satisfied. However, in the excitation of Eu^{2+} and the energy transfer from Eu^{2+} to Eu^{3+}, the admixing of the ground and the excited states, due to lattice vibration at high temperature, may allow the two transition probabilities to be relatively free from the spin selection rule.

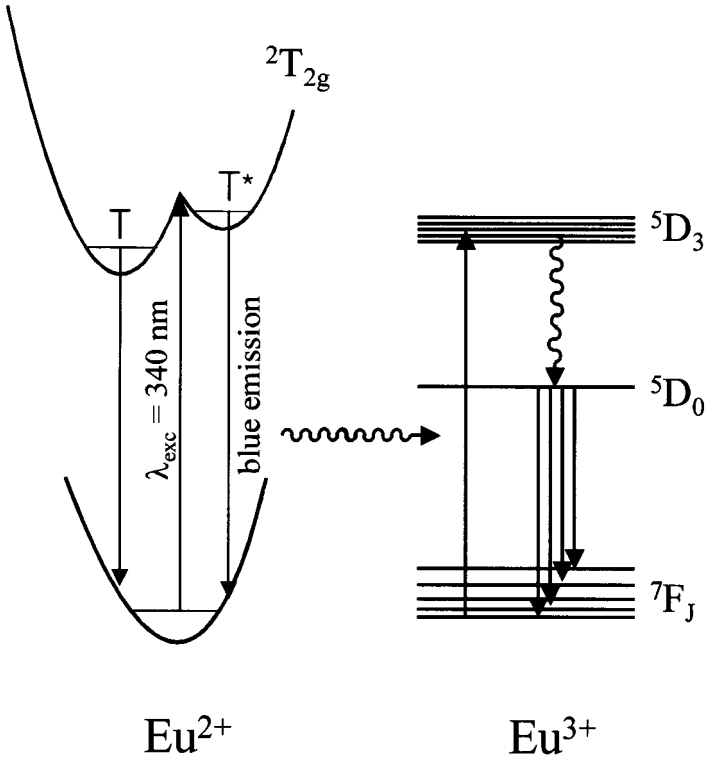

Figure 5. A schematic diagram of the induced luminescence from KCl resulting from the radiative energy transfer from Eu^{2+} to Eu^{3+} ions.

3.2. Luminescence from Eu^{3+}

The induced luminescence of Eu^{3+} via the radiative energy transfer consists of six processes, as shown in figure 5. The population at the $^5D_3$ level of Eu^{3+} increases via the radiative energy transfer from Eu^{2+} to Eu^{3+}. Finally, the population arrives at the emitting $^5D_0$ level via nonradiative transitions from the upper levels. The trivalent europium ion is very useful for studying the nature of metal coordination in various systems, owing to its non-degenerate emitting $^5D_0$ state. The crystal-field potential plays a key role in the optical process, which is characterized by site symmetry within the complex (Wybourne 1964, Morrison and Leavitt 1982, Hopkins *et al* 1996). The extent to which the $(2J + 1)$ degeneracy is removed depends upon the site symmetry of the Eu(III) ion. Furthermore, the number of observed bands in the

$^5D_0 \rightarrow {}^7F_J$ ($J = 2, 3, 4$) transitions is determined by the electric-dipole selection rule for a given point group. Under octahedral symmetry, $^5D_0 \rightarrow {}^7F_{0,2,3,4}$ transitions are forbidden by an electric dipole moment in principle. Groups of sharp lines indicate that the Eu^{3+} ion in KCl has a reduced site symmetry, rather than octahedral symmetry. The moderate intensity line peaking at 580.3 nm is attributed to the $^5D_0 \rightarrow {}^7F_0$ transition. For most Eu(III) complexes, this transition appears faintly. Surprisingly, the intensity of this transition is comparable with that of other lines. Possibly, the enhanced intensity is due to J mixing in low symmetries, such as C_s, C_n and C_{nv} (Bünzli 1989). Detailed information on the crystal field splitting can be obtained from the $^5D_0 \rightarrow {}^7F_1$ transition, since it accurately reflects the removal of $(2J + 1)$ degeneracy in the highly resolved luminescence. The $^5D_0 \rightarrow {}^7F_1$ transition, allowed by a magnetic dipole moment, has been observed with strong intensity independently of the environment. In general, the $^5D_0 \rightarrow {}^7F_1$ emission band can split into three components at most under symmetries lower than C_3 and C_{3v}. In the sample, the $^5D_0 \rightarrow {}^7F_1$ transition produces two strong bands, peaking at 588.1 and 596.0 nm. The strongest lines, peaking at 615.5 and 619.7 nm, were observed in the $^5D_0 \rightarrow {}^7F_2$ transition, exhibiting hypersensitivity. If the trivalent europium ion lies on an inversion centre, this hypersensitivity is absent. Furthermore, hypersensitivity can be presented when there is strong chemical bonding between Eu^{3+} ion and the environment. This suggests that the characteristic f $\rightarrow$ f emission from KCl may arise from localized EuOCl serving as an activator.

The two lines observed in the $^5D_0 \rightarrow {}^7F_2$ transition lead us to rule out point groups with horizontal or diagonal mirror-planes as possible site symmetries for the Eu^{3+} ion, since this transition can allow only one line or no lines under those reflections, respectively. The two very weak lines observed in the 650–660 nm region can be attributed to the $^5D_0 \rightarrow {}^7F_3$ transition, which is forbidden by an electric dipole moment. However, the J mixing of the $^7F_3$ state with other states may add an allowed magnetic dipole character, thereby increasing the intensity of the $^5D_0 \rightarrow {}^7F_3$ transition. This transition reveals the removal of the $(2J + 1)$ degeneracy to a certain extent, although the intensity is weak. Furthermore, the two observed lines, peaking at 651.6 and 654.8 nm, rule out point groups including a C_3 symmetry element. The C_{4v} point group is more plausible than the C_4 group for the site symmetry of Eu^{3+} for two reasons: more lines would be expected in the $^5D_0 \rightarrow {}^7F_3$ transition from C_4, and EuOCl itself has C_{4v} symmetry. The $^5D_0 \rightarrow {}^7F_4$ transition is sensitive to the ligand environment. As shown in figure 3, the intensity of this transition increased moderately. The characteristic feature of this transition is the three well separated luminescence lines, peaking at 686.6, 696.0 and 701.5 nm, rather than the enhanced intensity. The C_{4v} crystal-field potential primarily produces the four lines allowed by the electric dipole moment.

The crystal-field Hamiltonian (CFH) for the C_{4v} site-symmetry can be expressed in terms of spherical tensor operators $C_q^{(k)}$ as

$$H_{CF} = B_0^2 C_0^{(2)} + B_0^4 C_0^{(4)} + B_4^4 (C_{-4}^{(4)} + C_4^{(4)}) + B_0^6 C_0^{(6)} + B_0^6 (C_{-4}^{(6)} + C_4^{(6)})$$

where the CF parameter, B_q^k, represents the expansion coefficient. Assuming that the CFH does not cause mixing of ^7F_J and the other electronic states due to the large energy gap, the matrix elements in the CFH are approximated to the problems between the $|f^N {}^7F; J J_z\rangle$ and $|f^N {}^7F; J' J'_z\rangle$ states. According to the selection rule for the crystal quantum number (μ), the CF matrix elements between two states, $|f^N {}^7F; J J_z\rangle$ and $|f^N {}^7F; J' J'_z\rangle$, are nonzero if the two states have the same parity in the J_z quantum number (Wybourne 1964). Introducing this selection rule to the CFH, the full 48×48 set of matrix elements can be reduced to three sub-groups: $\mu = 0$ ($J_z = -4, 0, 4$), $\mu = \pm 1$($J_z = \mp 5, \pm 1, \mp 3$) and $\mu = 2(-2, 2)$.

In this work, we carried out CF simulation on the fine structures of the ^7F_J (J = 1–6) levels that arise from the C_{4v} crystal-field potential. The CF parameters and the barycentres

were determined by the best fit to the observed luminescence lines responsible for the $^5D_0 \rightarrow {}^7F_J (J = 0, 1, 2, 3, 4)$ transitions. The electric-dipole selection rule for the $^5D_0 \rightarrow {}^7F_J (J = 2, 3, 4)$ transitions under C_{4v} symmetry was employed to determine the fine set of CF parameters. The final values obtained for the CF parameters are $B_0^2 = 730(3)$, $B_0^4 = -400(3)$, $B_4^4 = \pm 590(10)$, $B_0^6 = 530(5)$ and $B_4^6 = \pm 845(5)$ cm^{-1}. In addition, the barycentres for $^7F_1$, $^7F_2$, $^7F_3$ and $^7F_4$ were obtained as 16 892, 16 239, 15 268, 14 282 cm^{-1}, respectively. Here, those for the $^7F_5$ and $^7F_6$ are 13 228 and 12 228 cm^{-1}, respectively, as calculated from the free-ion state (Kim *et al* 1998). The experimental and calculated luminescence lines are listed in table 1. This set of energy parameters produces a very good agreement between the observed and calculated luminescence lines within the root-mean-square deviation, $\sigma_{rms} = 3.1$ cm^{-1}.

Table 1. Experimental and calculated luminescence lines of Eu^{3+} under the C_{4v} site symmetry assigned to $^5D_0 \rightarrow {}^7F_J$ ($J = 0$, 1, 2, 3 and 4).[a]

No	J	Observed	Calculated[a]	Peak assignment $^5D_0(A_1) \rightarrow$
1	0	17 232	17 232	$^7F_0(A_1)$
2	1	17 003	17 009	$^7F_1(1E)$
		16 779	16 780	$^7F_1(A_2)$
	2		16 415	$^7F_2(1B)$
			16 251	$^7F_1(2B)$
3		16 247	16 250	$^7F_2(1E)$
4		16 137	16 135	$^7F_2(A_1)$
5	3	15 348	15 346	$^7F_3(2E)$
			15 338	$^7F_3(1B)$
6		15 273	15 276	$^7F_3(1E)$
			15 234	$^7F_3(A_2)$
			15 189	$^7F_3(2B)$
7	4	14 565	14 563	$^7F_4(1A_1)$
8		14 368	14 372	$^7F_4(1E)$
			14 295	$^7F_4(A_2)$
9		14 255	14 253	$^7F_4(2E)$
			14 227	$^7F_4(1B)$
			14 199	$^7F_4(2B)$
			14 124	$^7F_4(2A_1)$

[a] Satellite bands that appeared at the low- and high-energy edges of the main bands were not considered for assignment.

4. Conclusions

Distinct spectral holes appear in the blue emission from KCl co-doped with divalent and trivalent europium ions. The radiative energy transfer from Eu^{2+} to Eu^{3+} produces these holes and induces the $^5D_0 \rightarrow {}^7F_J$ ($J = 0$–4) luminescence lines of Eu^{3+}. The observed luminescence spectrum reflects the fact that the $(2J+1)$ degeneracy of Eu^{3+} is split into Stark sublevels by the crystal-field potential under the C_{4v} site symmetry. For the $J = 3$ state, the C_{4v} crystal-field potential splits the sevenfold degeneracy into five sublevels, 2E(∓ 3), 1B(-2 or 2), 1E(± 1), $A_2(0)$ and 2B(2 or -2), in order of increasing energy. The five observed holes reflect the transitions from the $^7F_0$ ground state to these five sublevels. As temperature decreases, the holes and the induced luminescence decrease and disappear below 50 K. A persistent spectral hole burnt on the $^7F_0 \rightarrow {}^5D_0$ excitation spectrum appears with weak intensity only at very low

temperatures with a high-power laser, while the strong spectral holes can be obtained with a UV lamp.

Alkali halide phosphors activated with colour centres have received spectroscopic attention as a host material. Specifically, alkali halides doped with divalent europium ion, emitting bright blue luminescence, have been recognized as suitable candidates for the active media of broadly tunable solid-state lasers and dosimetric applications. The co-dopants Eu^{2+} and Eu^{3+} might be useful for technological applications in view of their versatile spectroscopic properties.

Acknowledgments

This work was partially supported by Chungnam National University.

References

Buddhudu S, Morita M, Murakami S and Rau D 1999 *J. Lumin.* **83/84** 199
Bünzli J-C G 1989 *Lanthanide Probes in Life, Chemical and Earth Sciences* ed J-C G Bünzli and G R Choppin (Amsterdam: Elsevier) ch 7
Dexter D L 1953 *J. Chem. Phys.* **56** 2875
Fujita K, Hirao K, Tanaka K, Soga N and Sasaki H 1997 *J. Appl. Phys.* **82** 5114
Hopkins T D, Bolender J P, Metcalf D H and Richardson F S 1996 *Inorg. Chem.* **35** 5347
Kang J-G, Nah M-K and Sohn Y 2000a *J. Phys.: Condens. Matter* **12** L199
Kang J-G, Sohn Y, Nah M-K, Kim Y-D and Ogryzlo E A 2000b *J. Phys.: Condens. Matter* **12** 3485
Kim J-G, Yoon S-K, Sohn Y and Kang J-G 1998 *J. Alloys Compounds* **274** 1
Morrison C A and Leavitt R P 1982 *Handbook on the Physics and Chemistry of Rare Earths* vol 5, ed K A Gschneidner Jr and L R Eyring (Amsterdam: North-Holland) ch 46
Nogami M 1999 *J. Non-Cryst. Solids* **259** 170
Nogami M, Abe Y, Hirao K and Cho D H 1995 *Appl. Phys. Lett.* **66** 2952
Reisfeld R and Jörgensen C K 1977 *Lasers and Excited States of Rare Earths* (Berlin: Springer) ch 4
Rubio J O 1991 *J. Phys. Chem. Solids* **52** 101
Wybourne B G 1964 *Spectroscopic Properties of Rare Earths* (New York: Wiley)